EUROFUSION WPDIV-CP(16) 16509

P. Frosi et al.

Structural analysis of DEMO Divertor Cassette Body and design study based on RCC-MRx

Preprint of Paper to be submitted for publication in Proceedings of 29th Symposium on Fusion Technology (SOFT 2016)

This work has been carried out within the framework of the EUROfusion Consortium and has received funding from the Euratom research and training programme 2014-2018 under grant agreement No 633053. The views and opinions expressed herein do not necessarily reflect those of the European Commission.

Structural analysis of DEMO divertor cassette body and design study based on RCC-MRx

Paolo Frosi[a], Christian Bachmann[b], Giuseppe Di Gironimo[c], Giuseppe Mazzone[a], Domenico Marzullo[c], Jeong-Ha You[d]

a) Department of Fusion and Technology for Nuclear Safety and Security, ENEA C. R. Frascati, via E. Fermi 45, 00044 Frascati (Roma), Italy
b) EUROfusion, PPPT, Boltzmann Str. 2, 85748 Garching, Germany
c) CREATE Consortium/University of Naples Federico II, Department of Industrial Engineering (DII), Piazzale Tecchio 80 – 80125 Napoli, Italy
d) Max Planck Institute for Plasma Physics, Boltzmann Str. 2, 85748 Garching, Germany

This study is a part of the structural activity being conducted for developing European DEMO divertor in the framework of the EUROfusion Consortium. The thermal and structural analysis has already been started since a year and the first results had been partly published in a previous paper. The Cassette Body is being analyzed considering the most critical types of loads (e.g. coolant pressure, volumetric neutron heating and EM loads) according to their latest estimates. This work is based on the design-by-analysis approach adopted in the conceptual design study of the DEMO Divertor. The Divertor design has been assessed in terms of a number of variables e.g. loads, key geometric dimensions, positions of the Cassette attachments to the vacuum vessel, or position of load application, in order to enhance the knowledge about the structural behavior of the Divertor Cassette. In addition to the existing 3D solid element model, also a shell element model has been developed: so that an extensive parametric analysis can be easily done for a comparative estimation. The structural assessment was done according to the Design and Construction Rules for Mechanical Components of Nuclear Installation (RCC-MRx)

Keywords: fem, DEMO, Divertor, structural analysis, thermal analysis, RCC-MRx

1. Introduction

The present paper reports the latest progress in the structural design study for the European DEMO divertor cassette body which has been conducted in the framework of the work package “Divertor” of the EUROfusion Consortium [1-5]. The structural design study serves as one of the major elements of pre-conceptual design of DEMO divertor cassette. The structural design study is based on computational structural analysis and code-based design criteria. In the structural analysis multiple physical loads, which impose a major mechanical impact, should be taken into account. In this study, thermal loads from fusion plasma and neutronic heating, static loads by primary loads (e.g. coolant pressure, reaction force at supports) and dynamic loads due to electromagnetic forces are considered. The structural analysis is preceded by multi-physical analyses for load specification and followed by structural design assessment for which computed stress intensities are fed in into the design criteria. For effective stress analysis, the finite element models are optimized using different elements and meshing strategy. The structure of static supports is also optimized in an iterative process. As interim design rules, the criteria formulated in the French code RCC-MRx are employed in this preliminary study [6]. In this paper, the results of first round structural design study performed for DEMO divertor cassette body are presented. Besides a model using conventional 3D continuum solid element, an alternative model using parametric shell element is employed. Implications for further design optimization are discussed

2. Analysis with 3D fem model

The early analysis [1] has dealt with several simplifications: now some better approximations have been applied and they are going to be explained.

The most important improvement produced in the whole analysis has regarded the mesh: the solid model that initially was made up of only one volume has been divided in several connected parts to obtain the more confident mapped mesh as it can be seen in fig. 1.

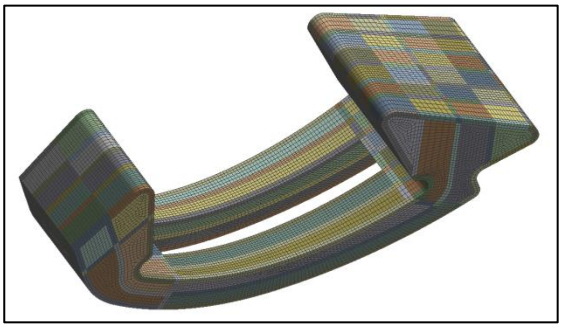

Fig. 1: mapped mesh of Cassette Divertor.

This action has been considered a priority for the progression of the study to give an overall enhancement to the reliability of the analysis. As usual, some preliminary attempts have been executed to choose a suitable element size. Finally a global size of 25 mm has been adopted and the model results with 71813 elements and 376473 nodes.

As reported in [1], it has been established that the Cassette is made of Eurofer whose physical properties

Corresponding author’s email: paolo.frosi@enea.it

can be found in [6]: also in [7] the same properties are reported: the values in both cases are practically equal. All the choices related to material modeling can be found in [1] and here they have been still adopted. The initial step of the study has regarded the thermal analysis: it essentially deals with neutron thermal power and convective cooling.

The first load value has been obtained from [8] in which a detailed subdivision of thermal power on each Divertor component has been described. The total thermal power on the 54 Cassettes (96.3 MW) must be divided for the number of Cassettes and for the volume of the single cassette (0.71866 m^3): it gives the thermal power per unit volume ($2.4737 \cdot 10^6$ W/m^3) that must be declared inside the model for the simulation of the internal heat generation. But in doing so the thermal power is applied uniformly: instead, as reported in [8], it really has a distribution with higher values in the inboard region and lower values in the outboard region; it hasn't been possible to consider such a distribution of neutron thermal power because the results haven't been supplied in a *table-formatted* manner.

The values related to convective cooling are: the convection film coefficient equals to 10 $kW/(m^2 \cdot K)$ like stated in [1] and the water bulk temperature equals to 210°C (it has been chosen conservatively the outlet value) according the last agreements (BoP) that aren't published yet. All the internal surfaces (reported in fig. 2) that are interested by convective and pressure loads have been clearly identified beforehand for the whole set of the following analysis.

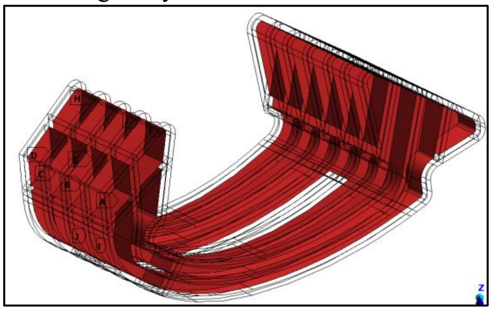

Fig. 2: internal surfaces for application of thermal and mechanical loads.

In doing so, the temperature distribution has been evaluated and it can be seen in fig.3.

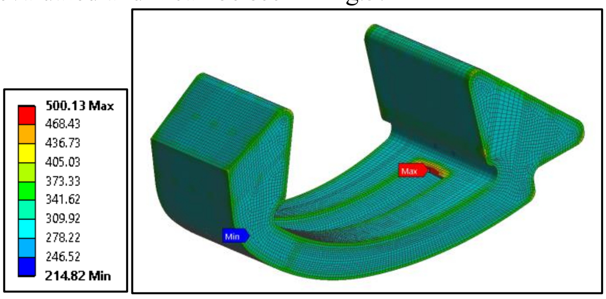

Fig. 3: contour plot of temperature (°C).

The peak values of temperature related to the sharp corners can be surely neglected because they can be weakened with a detailed dimensioning of the chamfers; the value of 309.92°C corresponding to the end of the third step in the legend can be chosen as representative of the state of the cassette and it isn't a dangerous level although the aforementioned uniform application of thermal loads. With this hypothesis, the thermal gradient inside the component and the following stresses arising from differential thermal expansion have been neglected. Nevertheless it must be kept in mind that it has been dealt with a steady state analysis that isn't far from the real situation in which the pulses are foreseen to last for several minutes: so the duration of the pulse turns in favour of a softening of these thermal gradients. In any case this point shall be engaged in the next paper.

The following step has regarded the structural analysis. The temperature distribution and the water pressure (whose value of 3.5 MPa comes from the same BoP mentioned above) have been applied having been defined the elastic-plastic kinematic hardening material model as in [1].

The resulting equivalent stresses have been reported in fig.4. These values are too high only at inwards corners that might be avoided with a detailed design of the sharp regions. For everything else, the values are less than yielding at the same temperature as proofed by plastic strain contour plot that is always zero (not reported).

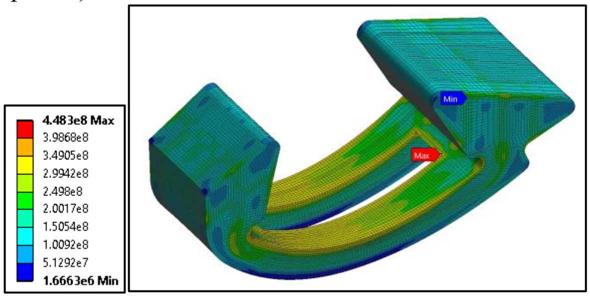

Fig. 4: equivalent stress for thermal and mechanical loads (Pa)

It is worth to be mentioned the study about the position of the attachments. The central, the intermediate and lateral regions have been chosen to perform some tests with different constraints (radial, toroidal and vertical displacements nullified by turns), in a symmetric and asymmetrical position. The solution that exhibits the lowest values of stress has been chosen and These positions of the attachments are reported in fig. 5.

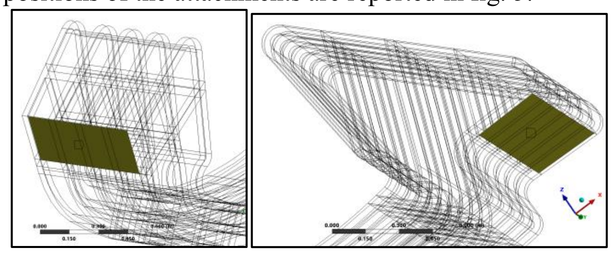

Fig. 5: inboard (left) and outboard (right) position of the attachments

The physical constraints that have been simulated are: radial, toroidal and vertical displacements nullified, then the rotations about radial and vertical axis have been nullified and finally the rotations about the toroidal direction have been kept free. This physical condition has been mathematically implemented using the Ansys tool named *remote point*: that is the above mentioned conditions on displacements and rotations have been declared on the centroids of the surfaces reported in fig. 5; in doing so these centroids act as *remote points*. This choice is seemed to be wise: in the fig. 6 the vertical displacements have been reported and it can be seen that the cassette is subjected to a flexural action that increases the curvature in its central region that is the most slender zone. So a certain quantity of strain energy has been stored in a slender zone and it keeps the stress values reasonably low.

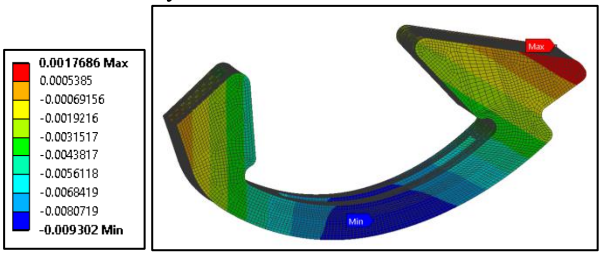

Fig. 6: vertical displacements of cassette (m)

But this result shall be reviewed because of the aforementioned uniform action of the neutron power: this distribution is expected to exercise a high flexural action that should straighten the curvature of the cassette and it should result in an important action on the attachments that can't be highlighted now.

As further demonstration of the severity of thermal loads, the fig. 7 reports the equivalent stresses related to the water pressure acting alone: it produces a very low level of stresses as already found in [1]

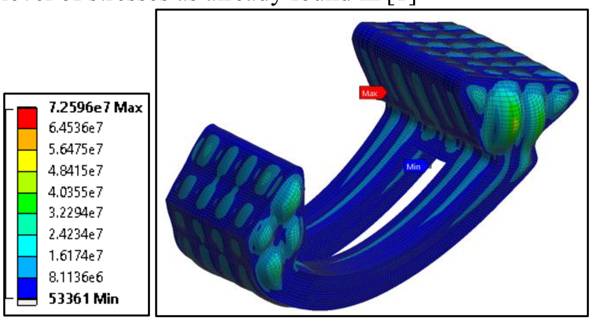

Fig. 7: equivalent stresses due to water pressure (Pa)

So the stresses reported in fig.4 are almost completely due to the thermal loads: this fact is confirmed by the case with thermal loads acting alone: here the Von Mises stresses (not reported) are almost equal to those ones in fig. 4. Moreover it is worth to mention that the maximum value in fig. 7 has been obtained in an inwards corner of the internal cooling volumes and other peak values can be found in similar regions: so once again a detailed design is required to avoid these singularities.

Another chapter of this study has regarded the influence of VDE event on this tokamak component. The first case is related to the study reported in [9], really related to Demo Divertor, in which the contribution of the halo currents to the EM forces has been evaluated. A forward step respect to [1] has been done: it is no more necessary to adopt the ITER values excluding any problem of translation and adaptation of that results; but also here it hasn't been possible to manage the real distribution of those forces: so the resultants (forces and moments) had to be divided uniformly on all nodes. The centroid of the cassette has been chosen as *remote point* and the lateral vertical surfaces have been associated to it to *spread* the resulting moments. The most severe case studied in [9] has been used and it is reported in tab.1.

Table 1. resultant forces (MN) and resultant moments (MNm) due to an heuristic case of halo currents.

F_{rad}	F_{tor}	F_{ver}	M_{rad}	M_{tor}	M_{ver}
2.72	0	5.70	0	45.4	0

In the fig. 8 there are the resulting equivalent stresses related to this case.

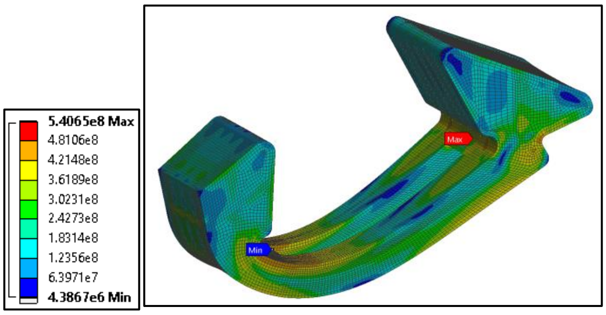

Fig. 8: equivalent stresses due to halo currents (Pa)

The stress level is higher than that reported in fig.4, and the plastic strains regard a zone a bit enlarged (not reported). Some refinements seem necessary according this case.

Another case of disruption has been taken from the most severe case reported in [10] with the simplified and uniform distribution of resultant forces and moments. The case extracted from this study has regarded the time at the end of the current quench. The values considered in this situation are reported in tab.2.

Table 2. resultant forces (MN) and resultant moments (MNm) due to an heuristic case of eddy and halo currents.

F_{rad}	F_{tor}	F_{ver}	M_{rad}	M_{tor}	M_{ver}
0.32	0.7	1	1.3	0.29	5.1

Now the state of stresses seems lower than the previous VDE case and comparable with the results in fig. 4. The fig. 9 reports the Von Mises stresses for this case.

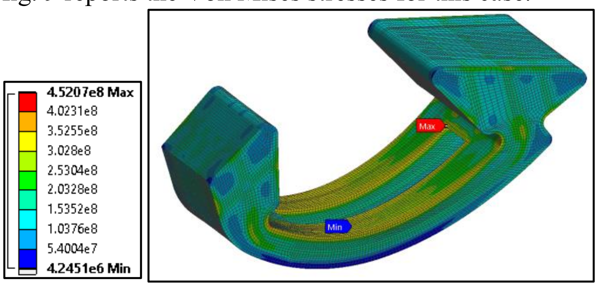

Fig. 9: equivalent stresses due to eddy and halo currents (Pa)

3. RCC-MRx simplified assessment

Even though the previous analysis has some uncertainty related to the load evaluation and the way of their application, a simplified application of basic statements of RCC-MRx code have been investigated. This set of analysis has been performed assuming a linear elastic behavior of the material. The line supporting segments have been chosen in the same position reported in [1]. In fig.10 these paths has been highlighted in a convenient virtual cut of the solid model.

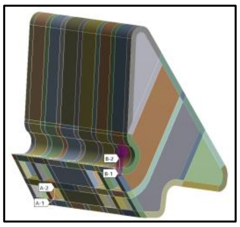

Fig. 10: path position for RCC-MRx assessment

The first step is to assure that membrane and bending stresses caused by mechanical load (water pressure) at its working temperature are below the allowable stresses at the same temperature. With clear symbolism (θ_m is the mean temperature along the path), in table 3 there is the summary of this point.

Table 3. assessment against primary damages

Path A1-A2	**Θm=339.34 °C**
P_m= 1.64 MPa	S_m = 185 MPa
$P_m + P_b$ = 2.9 MPa	$1.5{\cdot}S_m$ = 277 MPa
Path B1-B2	**Θm=315.5 °C**
P_m= 1.0 MPa	S_m = 189 MPa
$P_m + P_b$ = 4.33 MPa	$1.5{\cdot}S_m$ = 284 MPa

The second step has regarded then classical $3S_m$ rule that is the evaluation of the stress range from the stand-by condition (the component at the same temperature of water bulk value) to the maximum thermal stress condition that is with the full action of neutron thermal power. With the classical symbolism always used, in the tab. 4 the essential results have been reported.

Table 4. assessment against secondary damages

Path A1-A2	**Θm=339.34 °C**
Max(Pm + Pb)+ ΔQ = 109 MPa	3·Sm = 555 MPa
Path B1-B2	**Θm=315.5 °C**
Max(Pm + Pb)+ ΔQ = 238 MPa	3·Sm = 568 MPa

Also in this case as in [1], the simplified assessment has been satisfied.

4. Analysis with cassette shell model

The pre-conceptual design phase is an iterative design process aimed at developing different *concepts* that potentially meet the design requirements and analysing each concept in order to find the "best solution" [11]-[12]. In this phase, more than in the others, major changes occur constantly, thus a parametric design approach and the use of lighter FEA models are crucial to speed-up the whole design process, incorporating modifications to the models efficiently [13]-[14].

Divertor cassette parametric shell model (Fig. 11) is used to allow for optimization studies of ribs thickness and layout, taking into account coolant pressure, thermal loads and also cassette preloading needs. As first stage, comparative analyses with the 3D solid models presented in section 2 have been performed, applying the same boundary and load conditions.

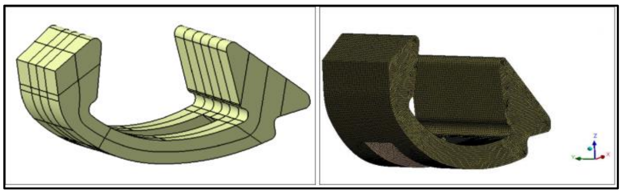

Fig. 11 Parametric Shell model from CATIA V5 to Ansys

In order to prepare future RCC-MRx assessment related to the shell model, both the Von Mises stress (middle) and the top/bottom Von Mises stresses have been obtained. To compare with the 3D results shown in section 2, the top/bottom results for the only coolant pressure and for the combination of coolant pressure and thermal loads are shown respectively in Fig. 12 and Fig. 13.

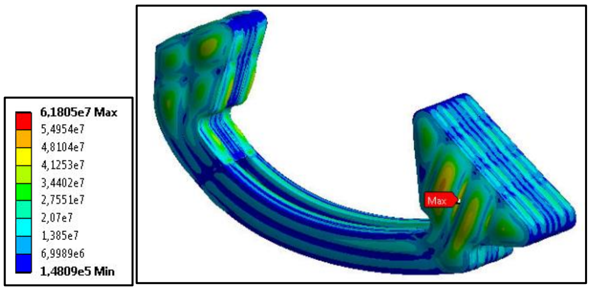

Fig. 12 Equivalent stress for coolant pressure load (top/bottom)

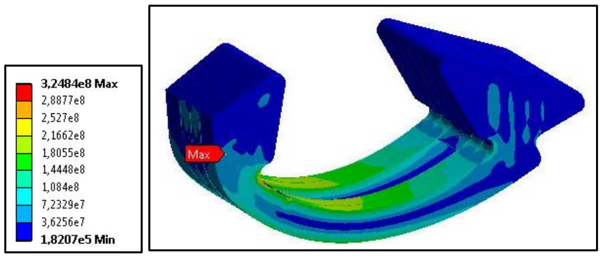

Fig.13 Equivalent stress for coolant pressure and thermal load (top/bottom)

Taking into account the obtained results, a first optimization process has been performed, in terms of ribs layout and thickness. The parametric approach allowed the implementation of modifications efficiently. In particular, the iterative analysis process shows the possibility to remove 2 poloidal ribs (see Fig. 14) and reduce the thickness from 40mm to 20mm.

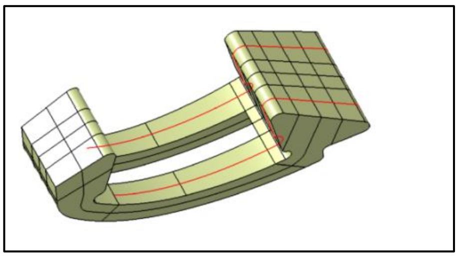

Fig. 14 Poloidal ribs removed

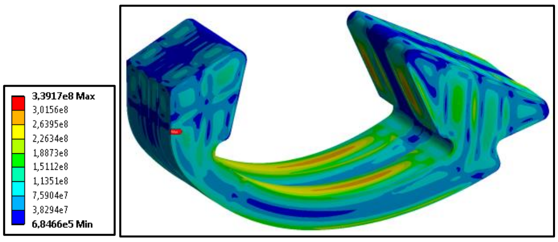

Fig. 15 Equivalent stress for coolant pressure and thermal load (top/bottom) with new ribs configuration

According to first structural analyses, thickness reduction and layout modification are acceptable against pressure and thermal loads. Furthermore the reduction in the cassette's stiffness allows for cassette preloading needed for locking and electrical needs.

Even though the maximum values of equivalent stresses and their positions in the 3D and 2D models are different, the distributions are similar and the order of magnitude agrees well in both cases. So further investigation related to the influence of the reduction of the ribs thickness on shielding performances and also their effects on the behaviour of the component against halo currents and EM loads can be carried on.

Conclusion

The structural analysis carried out for the reference model of DEMO divertor cassette body showed that the thermal power to be generated by nuclear heating would give the largest contribution to the final stress state. It was also confirmed that under the normal operation loads the structural failure criteria are not violated. The final judgment in terms of structural design feasibility can be made once the structural impact of off-normal dynamic loads due to electromagnetic forces (disruptions and vertical displacement events) has been assessed and evaluated against code rules. This work is ongoing.

Acknowledgments

This work has been carried out within the framework of the EUROfusion Consortium and has received founding from the European research and training program 2014-2018 under grant agreement N.633053. The views and opinions expressed herein do not necessarily reflect those of the European Commission.

References

[1] P. Frosi, G. Mazzone, Structural design of DEMO Divertor Cassette Body: provisional FEM analysis and introductive application of RCC-MRx design rules, Fusion Engineering and Design, 109-111 (2016) 47-51.

[2] F. Romanelli et al., Fusion electricity – a roadmap to the realization of fusion energy, (EFDA), ISBN 978-3-00-040720-8 (2012)

[3] G. Federici et al., Overview of EU DEMO design and R&D activities, Fusion Engineering and Design, 89 (2014) 882-889.

[4] C. Bachmann et al., Initial DEMO tokamak design configuration studies, Fusion Engineering and Design, 98-99 (2015) 1423-1426.

[5] J.H. You et al., Conceptual design studies for the European DEMO Divertor. Rationale and first results, Fusion Engineering and Design, 109-111 (2016), 1598-1603.

[6] RCC-MRx 2012 AFCEN Edition, Design and Construction Rules for Mechanical Components of Nuclear Installation.

[7] Material Property Handbook pilot project On EUROFER97, EFDA_D-2MRP77

[8] R. Villari et al., Neutron Analysis Report for Divertor Cassette and PFC, EFDA_D_2MN6FV

[9] V. Cocilovo, EM Analysis Report for Divertor Cassette Body, EFDA_D_2MZGPJ

[10] M. Roccella et al., Development of global EM analysis model, EFDA_D_2MMBW

[11] Di Gironimo, G., et al. Iterative and Participative Axiomatic Design Process in complex mechanical assemblies: case study on fusion engineering. International Journal on Interactive Design and Manufacturing (IJIDeM) 9.4 (2015): 325-338.

[12] Di Gironimo, G., et al. Concept design of the DEMO divertor cassette-to-vacuum vessel locking system adopting a systems engineering approach. Fusion Engineering and Design 94 (2015): 72-81.

[13] Mozzillo, R., et al. "Development of a master model concept for DEMO vacuum vessel." Fusion Engineering and Design (2016).

[14] Marzullo, Domenico, et al. "Design progress of the DEMO divertor locking system according to IPADeP methodology." *Procedia CIRP* 34 (2015): 56-63.